

Anomalous Modes Drive Vortex Dynamics in Confined Bose-Einstein Condensates

David L. Feder,^{1,2} Anatoly A. Svidzinsky,³ Alexander L. Fetter,³ and Charles W. Clark²

¹Clarendon Laboratory, University of Oxford, Parks Road, Oxford OX1 3PU, United Kingdom

²Electron and Optical Physics Division, National Institute of Standards and Technology, Technology Administration, United States Department of Commerce, Gaithersburg, Maryland 20899-8410

³Laboratory for Advanced Materials and Department of Physics, Stanford University, Stanford, California 94305-4045
(Received 5 September 2000)

The dynamics of vortices in trapped Bose-Einstein condensates are investigated both analytically and numerically. In axially symmetric traps, the critical rotation frequency for metastability of an isolated vortex coincides with the largest vortex precession frequency (or anomalous mode) in the Bogoliubov excitation spectrum. The number of anomalous modes increases for an elongated condensate. The largest mode frequency exceeds the thermodynamic critical frequency and the nucleation frequency at which vortices are created dynamically. Thus, anomalous modes describe both vortex precession and the critical rotation frequency for creation of the first vortex in an elongated condensate.

DOI: 10.1103/PhysRevLett.86.564

PACS numbers: 03.75.Fi, 05.30.Jp, 32.80.Pj

Bose-Einstein condensation (BEC) and superfluidity are two entangled core issues of low-temperature physics, and recent experimental developments now allow us to study them in a nearly ideal system: a dilute gas of alkali atoms with well-understood interactions [1–3]. Many key aspects of BEC have been clarified since the first experimental observations, and during the past year much attention has been given to manifestations of superfluidity. The “scissors mode” of excitation of trapped condensates [4] implies the irrotational flow characteristic of superfluids. Quantized vortices, which have long been known as fundamental excitations of superfluid helium and superconductors, have been observed directly in one- [5,6] and two-component [7] trapped Bose gases.

Multiple vortices have recently been generated in confined single-component condensates [5] by rotating a weakly anisotropic trap at an angular frequency Ω . This approach resembles the classic rotating-bucket experiments on liquid helium [8], where vortices first appear [9] at a critical frequency Ω_c above which the presence of the vortex lowers the total free energy [10,11]. There is a discrepancy, however, between the observations of Madison *et al.* [5] and simple theoretical considerations based on the equilibrium solution of the Gross-Pitaevskii (GP) equation, which has otherwise been remarkably successful in describing condensate behavior [1]; in particular, the frequency at which vortices are first observed is significantly higher than equilibrium estimates of Ω_c .

The resolution of this discrepancy is the subject of the present paper. In particular, we find that the “anomalous modes” of the Bogoliubov spectrum determine the critical rotation frequencies at which vortex arrays are observed in the ENS experiment [5]; they also determine the frequency of precession of the vortex core observed at JILA [6].

In trapped condensates, several factors influence the critical rotation frequency for appearance and stability of vortices, and for their subsequent dynamical motion.

(1) An energy barrier at the surface of the condensate [12] inhibits vortex penetration of its interior. Thus, vortices are predicted to nucleate spontaneously at a frequency $\Omega_\nu > \Omega_c$ [13], whose value coincides with the criterion for the Landau instability of surface excitations [14–16] and with the effective disappearance of the surface barrier [13]. We show below that, while Ω_ν exceeds Ω_c for the cigar geometry of the ENS experiments [5], it is still lower than the frequency at which vortices are first observed.

(2) Stringari [17] has shown that Ω_c increases with T , reaching a maximum close to the BEC transition T_c . The temperature $T \sim 0.8T_c$ required to match the observed critical frequency, however, is much larger than the temperature at which the experiments are performed.

(3) A condensate with a vortex first becomes stable against small perturbations at the metastability frequency Ω_m . One definition for metastability is that the energy per particle must not decrease under infinitesimal displacements of the vortex from the condensate center; for a disk-shaped condensate, this yields $\Omega_m = \frac{3}{5}\Omega_c$ in the Thomas-Fermi (TF) limit [12]. Equivalently, the Bogoliubov excitation spectrum must contain only modes with positive energy. A nonrotating axisymmetric condensate with a singly quantized vortex has at least one “anomalous mode”; such modes have a negative excitation energy ε_a and a positive norm [18,19]. For a rotating axisymmetric trap, these anomalous modes are Doppler-shifted upward by Ω , with the metastability frequency $\Omega_m = \max(|\varepsilon_a|)/\hbar$. As shown below, Ω_m can exceed both Ω_c and Ω_ν in cigar traps.

This criterion for the onset of linear stability agrees well with the large frequency at which vortices first appear experimentally in cigar-shaped condensates [5]. It also explains why the observed critical frequency is independent of whether the condensate is first cooled and subsequently rotated, or *vice versa*. Otherwise, the critical rotation should be greater for the cool-and-then-rotate

scenario, since vortices must surmount the energy barrier at the condensate surface, penetrating the cloud only at the nucleation frequency $\Omega_\nu > \Omega_c$.

(4) The anomalous modes correspond to the precession of the vortex core about the origin of the trap [12,20]. For $\Omega < \Omega_m$, the vortex moves in the same direction as the superfluid flow around the core. Hence, the anomalous mode(s) should describe the motion of one-component vortices in recent JILA experiments [6,7].

The present work links anomalous modes with these various observations. We proceed from the zero-temperature description of the order parameter (or wave function) for a condensate of ^{87}Rb atoms, as a solution to the time-dependent GP equation

$$i\partial_t\psi(\mathbf{r},t) = (T + V_{\text{trap}} + V_{\text{H}} - \Omega L_z)\psi(\mathbf{r},t), \quad (1)$$

with the kinetic energy operator given by $T = -\frac{1}{2}\vec{\nabla}^2$, the Hartree field by $V_{\text{H}} = 4\pi\eta|\psi|^2$, and trap potential by $V_{\text{trap}} = \frac{1}{2}[\lambda^2(1 + \epsilon_x)x^2 + \lambda^2(1 + \epsilon_y)y^2 + z^2]$, where $\lambda = \omega_\rho/\omega_z$ is the trap anisotropy and ϵ_x, ϵ_y describe (small) departures of the trap from axial symmetry. The centrifugal term $-\Omega L_z = i\Omega(x\partial_y - y\partial_x)$ appears for systems rotating about the z axis at a frequency Ω . Energy, length, and time are, respectively, given in harmonic oscillator units $\hbar\omega_z$, $d_z = \sqrt{\hbar/M\omega_z}$, and ω_z^{-1} , where ω_z is the axial trap frequency and M is the atomic mass. Normalizing the condensate wave function $\int d\mathbf{r} |\psi(\mathbf{r},t)|^2 = 1$ yields the scaling parameter $\eta = Na/d_z$, where $a = 100a_0 \approx 5.29$ nm is the ^{87}Rb scattering length [21] and N is the number of condensate atoms. As parameters typical of the recent experiments at ENS [5] and JILA [6,7], we take $N = 1.4 \times 10^5$ with $(\nu_\rho, \nu_z) = (\omega_\rho, \omega_z)/2\pi = (169, 11.7)$ Hz and $(\epsilon_x, \epsilon_y) = (0.03, 0.09)$, and $N = 3 \times 10^5$ with $(7.8, 7.8)$ Hz and $\epsilon_x = \epsilon_y = 0$, respectively.

The stationary solutions of the GP equation, defined as local minima of the free energy, are found numerically by norm-preserving imaginary time propagation using an adaptive stepsize Runge-Kutta integrator. The spatial dependence of the complex condensate wave function employs a discrete-variable representation [22] based on Gaussian quadrature, and is assumed to be even under inversion of z . The numerical techniques are described in greater detail elsewhere [13,22]. The initial condensate amplitude is taken to be the TF wave function $\psi_{\text{TF}} = \sqrt{(\mu_{\text{TF}} - V_{\text{trap}})/4\pi\eta}$, where $\mu_{\text{TF}} = \frac{1}{2}(15\lambda^2\eta)^{2/5}$ is the chemical potential. The GP equation for a given value of Ω and N is propagated in imaginary time until the fluctuations in both the chemical potential and the norm become smaller than 10^{-11} .

Once the system reaches equilibrium, its response to small disturbances is found by substituting $\psi \rightarrow e^{-i\mu t}(\psi + ue^{-i\epsilon t} + ve^{i\epsilon t})$ in Eq. (1). The Bogoliubov spectrum of eigenvalues ϵ is found by linearizing in the quasiparticle amplitudes $u(\mathbf{r})$ and $v(\mathbf{r})$.

Figure 1 shows the critical frequency $\Omega_c/2\pi$ and the nucleation frequency $\Omega_\nu/2\pi$ as a function of trap anisotropy λ . We ignore the small in-plane trap distortion (setting $\epsilon_x = \epsilon_y = 0$) in order to simplify the computation. In this axisymmetric system, the thermodynamic critical frequency Ω_c is the energy difference between condensates with and without a vortex at the trap center (divided by \hbar), since the rotation Doppler shifts the former by exactly $-\Omega$; for the parameters of the ENS experiment, $\lambda \approx 14.44$, we obtain $\Omega_c/2\pi \approx 0.4\nu_\rho \approx 68$ Hz, in good agreement with the TF estimate but much lower than the observed value $\Omega_{\text{obs}}/2\pi \approx 0.7\nu_\rho \approx 120$ Hz. We find that inclusion of the small in-plane anisotropy does not appreciably increase the value of Ω_c , in contrast with results reported recently [23]. The critical nucleation frequency $\Omega_\nu = \min(\epsilon_{nm}/\hbar m)$ defines the rotation frequency at which the first Bogoliubov excitation of the vortex-free condensate becomes unstable [14]. We obtain $\Omega_\nu/2\pi \approx 0.52\nu_\rho \approx 88$ Hz, which is larger than $\Omega_c/2\pi$ but still too low to account for the experimental result.

Also shown in Fig. 1 are the frequencies of the anomalous modes $|\omega_a|/2\pi = |\epsilon_a|/\hbar$ with even z parity (plotted as positive values). These are Bogoliubov excitations of the vortex state with negative energy but positive norm, and relative angular momentum $-\hbar$. For spherical or pancake geometries, the spectrum contains only one anomalous mode. It describes the precession of the vortex about the center of the trap, in the same sense as the circulation about the core [20] at a frequency $\omega_a = \frac{3}{5}\Omega_c$ in the TF limit [12]. As λ increases and the vortex line stretches, however, additional anomalous modes appear in the energy

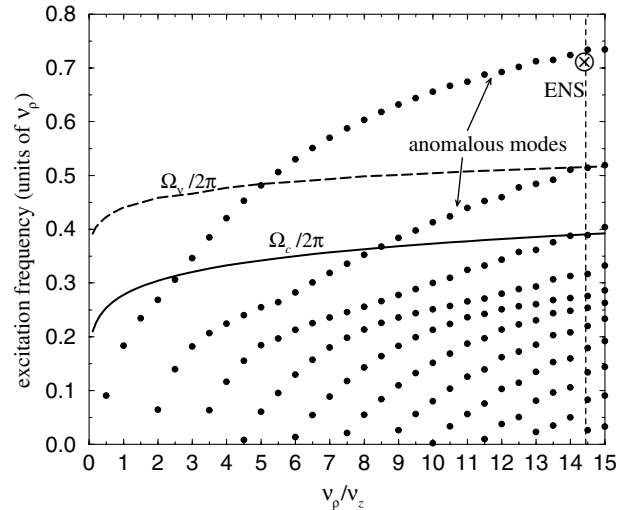


FIG. 1. The numerical values for the thermodynamic critical frequency $\Omega_c/2\pi$ (solid curve), the nucleation frequency $\Omega_\nu/2\pi$ (dashed curve), and the even z -parity anomalous mode frequencies (circles) are shown as a function of trap anisotropy $\lambda = \nu_\rho/\nu_z$. Parameters are $N = 1.4 \times 10^5$, $\nu_z = 11.7$ Hz, and $\epsilon_x = \epsilon_y = 0$. The dotted vertical line corresponds to anisotropy relevant to the ENS experiments, and the “ \otimes ” labels the frequency at which vortices are first observed.

spectrum [24,25], corresponding to the precession of a spatially deformed vortex line. Physically, Ω_c involves only a straight vortex (note, however, that Ref. [23] finds a deformed vortex for the ground state in very elongated condensates), but Ω_m involves linearized deformations. For an elongated condensate ($\lambda \gg 1$), the large curvature of the condensate surface readily induces distortions. The Bogoliubov amplitudes are highly localized radially in the vortex core and oscillate as a function of z , with maximum amplitude near the condensate surface. In the TF limit, n anomalous modes appear above a critical anisotropy $\lambda_n \geq \sqrt{n(n+1)}/2$ [25].

Excitation of the anomalous modes can lower the system's free energy, destabilizing the vortex state. Metastability of the vortex is guaranteed for rotation frequencies exceeding the largest anomalous mode, $\Omega_m = \max(|\omega_a|)$. In the TF limit, Ω_m exceeds Ω_c when $\lambda > 2$ [25], which is close to the value of $\lambda \approx 2.5$ found numerically (see Fig. 1). When such elongated condensates rotate with $\Omega_c < \Omega < \Omega_m$, the straight vortex line along the z axis can lower its energy by undergoing a finite-amplitude deformation. The ground state corresponds to a curved vortex displaced from the z axis [23,25], but experiments have not detected these states. For the ENS parameters, numerical analysis finds the metastability critical frequency $\Omega_m/2\pi = 0.73\nu_\rho \approx 124$ Hz, very close to the observed value $\Omega_{\text{obs}}/2\pi \approx 120$ Hz.

For the spherical trap relevant to the JILA experiments, the anomalous mode frequency in the TF limit has the predicted form $|\omega_a|/\omega = \frac{8}{5}(\xi/R) \ln(1.96R/\xi)$, if we neglect terms of relative order $(\xi/R) \ln(R/\xi) \approx 0.1$, where $R = (15\eta)^{1/5}$ is the TF radius and $\xi = 1/R$ is the dimensionless healing length. We find $|\omega_a|/2\pi = 1.58 \pm 0.16$ Hz, in reasonable agreement with the observed precession frequency of 1.8 ± 0.1 Hz. The value of $|\omega_a|$, however, is sensitive to the number of condensate atoms ($\propto N^{-2/5}$) and the displacement of the vortex from the trap center [26] ($\propto [1 - (\rho/R)^2]^{-1}$). Note that the JILA observations confirm the predicted negative sign of the anomalous frequency, for the vortex is seen to precess in the same sense as the superfluid flow around the core. Interestingly, the spectrum computed numerically also contains a *counterprecessing* (i.e., nonanomalous) mode with frequency 3.63 Hz and two nodes along z ; this may correspond to the distorted "rogue" vortices observed in two-component systems [6].

To make closer contact between vortex precession and anomalous Bogoliubov modes, the dynamics of a trapped vortex are explored by real-time propagation of the GP equation (1). Once the ground state has been obtained, an off-center vortex with counterclockwise circulation is imposed on the condensate wave function at $t = 0$ by the method of phase imprinting [27]. The vortex is displaced by $1.57d_\rho$ along \hat{x} from the trap origin, corresponding to $1.3 \mu\text{m}$ and $6.1 \mu\text{m}$ for the ENS and JILA condensates, respectively. In both cases, the vortices undergo counter-

clockwise precession, which is the same sense as the circulation around the vortex core.

For the JILA parameters, the period is found to be 623 ± 3 ms (the uncertainty reflects the coarseness of the spatial and temporal grids), yielding a precession frequency of $\omega_p/2\pi = 1.61 \pm 0.01$ Hz in excellent agreement with the value of the predicted anomalous-mode frequency discussed above. The phonons that are also produced by phase imprinting [27] only weakly affect the vortex motion, and they rapidly decay into unobservable high-frequency collective modes. The vortex itself is slightly curved, as discussed in Ref. [25]. No noticeable variation in the vortex displacement from the trap center (spiraling) was found after three full precessions.

As shown in Fig. 2, precession of an off-center vortex in the ENS trap is associated with a pronounced curvature of the vortex line. The precession appears to be most rapid near the surface of the condensate; by 12 ms, the ends of the vortex have returned to their initial location, while the center lags behind by almost 180° . Defining the precession by the motion near the surface, one obtains a frequency of approximately 85 Hz. This value (and to some extent the shape of the vortex) is consistent with the second-largest anomalous mode in the excitation spectrum shown in Fig. 1, $|\omega_a|/2\pi = 0.51\nu_\rho \approx 87$ Hz, which has two nodes along z . The excitation of this precession mode probably arises from imprinting a circulation pattern aligned with the z axis on a condensate

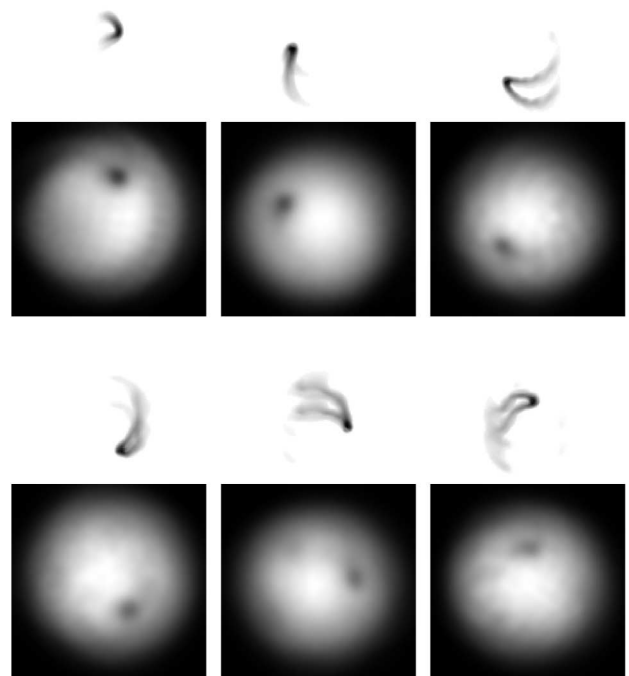


FIG. 2. Numerical simulation for the precession of a vortex in the ENS trap. Frames in raster order correspond to 4 ms increments after the initial phase imprint. Square panels, which are $8d_\rho \approx 6.7 \mu\text{m}$ on a side, show the integrated density down \hat{z} ; the corresponding vortex line (viewed 9° off the z axis toward $-\hat{y}$) is rendered above each frame.

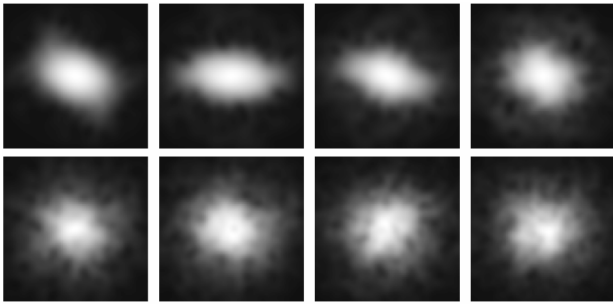


FIG. 3. Numerical simulation for a condensate in the ENS trap that starts rotating at $\Omega = 0.8\omega_\rho$ at $t = 0$. Images in raster order correspond to 150 ms through 500 ms in 50 ms increments, and are each $10\ \mu\text{m} \times 10\ \mu\text{m}$. The condensate density (integrated down \hat{z}) is shown in the rotating frame.

that is highly nonuniform radially; the initial straight vortex would have some overlap with all of the 11 even z -parity negative-energy modes found above for this configuration.

The critical frequency for vortex nucleation in elongated traps is confirmed by numerical solution of the time-dependent GP equation. The initially axisymmetric ENS condensate is simultaneously distorted ($\epsilon_x, \epsilon_y \neq 0$) and rotated at $t = 0$. The GP equation is propagated in the rotating frame for 500 ms with either $\Omega = 0.7\omega_\rho$ or $0.8\omega_\rho$. No vortices are produced for the $\Omega = 0.7\omega_\rho$ case. As shown in Fig. 3, however, when $\Omega = 0.8\omega_\rho$ vortices appear at the condensate surface by $t = 200$ ms, and fully penetrate the cloud by $t = 300$ ms. In the absence of dissipation, the vortex motion remains extremely turbulent; the dynamics of nucleating vortices will be addressed in greater detail elsewhere [28]. In the ENS experiment, the condensates are held for 500 ms. The reproducibility of those observations suggests that the vortex structures may have approached equilibrium through some dissipative process such as interaction of the condensate with the thermal cloud [29]; our simulations omitted such processes.

For an anisotropic trap with $\epsilon_x \neq \epsilon_y$, the anomalous mode $\omega_a(\Omega)$ becomes imaginary in the range $|\omega_a| - \delta \lesssim \Omega \lesssim |\omega_a| + \delta$, where $2\delta = |\epsilon_x - \epsilon_y|$ [25]. The onset of metastability in such traps occurs only when Ω exceeds $|\omega_a|$ by the appropriate amount, which may help explain the relevance of $\Omega_m \gtrsim |\omega_a|$ for the ENS experiments.

In summary, anomalous modes are interpreted as defining both the vortex precession in the JILA experiments [6] and the critical frequency for the appearance of the first vortex in the ENS experiments [5].

The authors are grateful to B. P. Anderson, E. A. Cornell, J. Dalibard, J. Denschlag, and S. L. Rolston for numerous fruitful discussions. This work was supported in part by the U.S. office of Naval Research, by NSF Grant No. DMR 99-71518, and by Stanford University.

- [1] A. S. Parkins and D. F. Walls, Phys. Rep. **303**, 1 (1998); F. Dalfovo, S. Giorgini, L. Pitaevskii, and S. Stringari, Rev. Mod. Phys. **71**, 463 (1999).
- [2] *Bose-Einstein Condensation in Atomic Gases*, edited by M. Inguscio, S. Stringari, and C. E. Wieman (IOS Press, Amsterdam, 1999).
- [3] See <http://amo.phy.gasou.edu/bec.html> for information on recent experiments.
- [4] D. Guéry-Odelin and S. Stringari, Phys. Rev. Lett. **83**, 4452 (1999); O. M. Maragò *et al.*, Phys. Rev. Lett. **84**, 2056 (2000).
- [5] K. W. Madison, F. Chevy, W. Wohlleben, and J. Dalibard, Phys. Rev. Lett. **84**, 806 (2000); K. W. Madison, F. Chevy, W. Wohlleben, and J. Dalibard, J. Mod. Opt. **47**, 2715 (2000); F. Chevy, K. W. Madison, and J. Dalibard, Phys. Rev. Lett. **85**, 2223 (2000).
- [6] B. P. Anderson, P. C. Haljan, C. E. Wieman, and E. A. Cornell, Phys. Rev. Lett. **85**, 2857 (2000).
- [7] J. E. Williams and M. J. Holland, Nature (London) **401**, 568 (1999); M. R. Matthews *et al.*, Phys. Rev. Lett. **83**, 2498 (1999).
- [8] R. J. Donnelly, *Quantized Vortices in Helium II* (Cambridge University Press, Cambridge, 1991).
- [9] R. E. Packard and T. M. Sanders, Jr., Phys. Rev. Lett. **22**, 823 (1969); Phys. Rev. A **6**, 799 (1972).
- [10] G. A. Williams and R. E. Packard, Phys. Rev. Lett. **33**, 280 (1974); E. J. Yarmchuck, M. J. V. Gordon, and R. E. Packard, *ibid.* **43**, 214 (1979); E. J. Yarmchuck and R. E. Packard, J. Low Temp. Phys. **46**, 479 (1982).
- [11] A. L. Fetter, J. Low Temp. Phys. **16**, 533 (1974).
- [12] A. L. Fetter, Int. J. Mod. Phys. B **13**, 643 (1999); A. A. Svidzinsky and A. L. Fetter, Phys. Rev. Lett. **84**, 5919 (2000); A. L. Fetter, in Ref. [2], pp. 201–263.
- [13] D. L. Feder, C. W. Clark, and B. I. Schneider, Phys. Rev. A **61**, 011601 (2000).
- [14] F. Dalfovo *et al.*, Phys. Rev. A **56**, 3840 (1997).
- [15] U. Al Khawaja, C. J. Pethick, and H. Smith, Phys. Rev. A **60**, 1507 (1999).
- [16] T. Isoshima and K. Machida, Phys. Rev. A **60**, 3313 (1999).
- [17] S. Stringari, Phys. Rev. Lett. **82**, 4371 (1999).
- [18] R. J. Dodd, K. Burnett, M. Edwards, and C. W. Clark, Phys. Rev. A **56**, 587 (1997).
- [19] D. S. Rokhsar, Phys. Rev. Lett. **79**, 2164 (1997).
- [20] M. Linn and A. L. Fetter, Phys. Rev. A **61**, 063603 (2000).
- [21] P. S. Julienne, F. H. Mies, E. Tiesinga, and C. J. Williams, Phys. Rev. Lett. **78**, 1880 (1997).
- [22] B. I. Schneider and D. L. Feder, Phys. Rev. A **59**, 2232 (1999).
- [23] J. J. García-Ripoll and V. M. Pérez-García, e-print cond-mat/0006368.
- [24] J. J. García-Ripoll and V. M. Pérez-García, Phys. Rev. A **60**, 4864 (1999).
- [25] A. A. Svidzinsky and A. L. Fetter, Phys. Rev. A **62**, 063617 (2000).
- [26] E. Lundh and P. Ao, Phys. Rev. A **61**, 063612 (2000).
- [27] J. Denschlag *et al.*, Science **287**, 97 (2000).
- [28] D. L. Feder, P. Ketcham, and C. W. Clark (unpublished).
- [29] P. O. Fedichev and G. V. Shlyapnikov, Phys. Rev. A **60**, R1779 (1999).